

Impulse waves at Kühtai reservoir generated by avalanches and landslides

H. Fuchs & R.M. Boes

Laboratory of Hydraulics, Hydrology and Glaciology (VAW), ETH Zurich, Zurich, Switzerland

M. Pfister

Laboratory of Hydraulic Constructions (LCH), Ecole Polytechnique Fédérale de Lausanne (EPFL), Lausanne, Switzerland. Formerly: VAW, ETH Zurich

ABSTRACT: The Kühtai reservoir is planned as an addition to the existing Sellrain-Silz group of HPPs. Two natural hazards relevant in terms of potential impulse wave impact on the dam were identified: a snow avalanche near the dam axis and a possible landslide further upstream. A preliminary analytical evaluation of impulse wave heights and wave run-up based on empirical equations showed that dam overtopping could not be excluded. However, several limitations of this evaluation were not satisfied, resulting in a reduced validity of the prediction. Thus, impulse wave generation was investigated in a 1:130 hydraulic scale model. Beside tests related to the relevant events, an additional systematic parameter variation validated the quality of the results. However, as no overtopping occurred even for the parameter variation, no measures such as breakwater or increase of the freeboard were required. The model test results are compared to a further analytical evaluation based on the recently published VAW-manual on landslide generated impulse waves.

1 INTRODUCTION

In addition to the existing Sellrain-Silz group of HPPs the Kühtai reservoir is currently planned by the Tyrolean Hydropower Company TIWAG-Tiroler Wasserkraft AG in order to increase the total storage volume (Boes et al. 2007). During load determination, two hazards relevant in terms of potential impulse wave impact on the 140 m high dam were identified (Fig. 1):

1. A snow avalanche zone close to the dam axis. Since the reservoir is located in the Alps at high altitude, intense snowfall and steep topography may result in a variety of avalanche events possibly impinging the reservoir. Governing avalanche parameters were evaluated by numerical simulations and provided by TIWAG. The gross avalanche volume was estimated to 90,000 m³.
2. An unstable jointed beak of rock about 300 m upstream of the dam possibly provoking landslides. A survey and evaluation of rock fissures resulted in two possible failure scenarios, one with a gross volume of 5000 m³ and another with 10,000 m³ slightly further upstream. Both are initiated directly above the full supply water level (FSL). For further comparisons only the scenario generating larger waves will be considered hereafter.

Both events are expected to transmit a certain impulse to the water and thus generate impulse waves when impinging the reservoir. A preliminary estimation of the expected waves resulted in a possibility for dam-overtopping, representing a potential dam safety risk. The Laboratory of Hydraulics, Hydrology and Glaciology (VAW) was therefore assigned to physically model relevant avalanche and landslide impact into a laboratory scale reservoir.

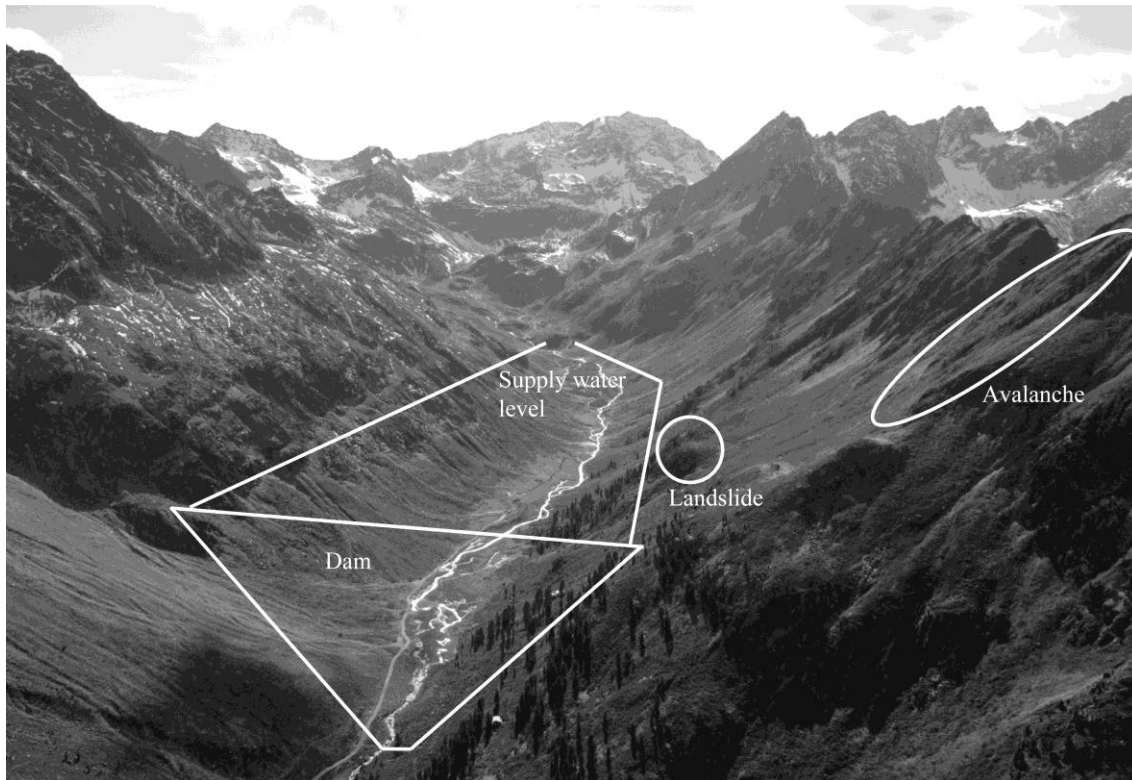


Figure 1. Planned Kühtai reservoir including dam contour, full supply water level and landslide as well as avalanche zones (courtesy of TIWAG).

2 PHYSICAL MODEL

The 1:130 physical scale model includes the complete dam, both valley flanks and roughly half of the reservoir length (Fig. 2). The model thus represents a 500 m wide and 600 m long section of the prototype. The complete height reaches from the reservoir bottom at 2030 m a.s.l. up to an elevation of 2200 m a.s.l., i.e. 60 m above FSL. The FSL is defined at an elevation of 2140 m a.s.l., thereby ensuring a freeboard of 5.0 m along the dam crest at 2145 m a.s.l. With a reservoir depth of 110 m, equivalent to a model depth of 0.85 m, relevant scale effects regarding wave generation and propagation are small (Heller et al. 2008, Dean & Dalrymple 2008). To reduce wave reflections and thus avoid model effects a wave absorber is located at the upstream model boundary corresponding to roughly half of the prototype reservoir length. The spillway located at the left dam embankment has been modeled only qualitatively including an increased hydraulic capacity, since the model scale did not allow for correctly scaled flow conditions. The volume of the unsteady spillway flow was determined by continuously weighing the impulse wave induced discharge.

The avalanche was modeled using a generator-chute hinged on top of the left model valley flank. With variable bottom slope, generator-flap elevation and opening a large variety of avalanche parameters could be generated. A granulate material consisting of white polypropylene (PP) with a grain diameter of 2 to 3 mm was filled in the load zone behind the generator-flap. With a porosity of 39% the grain density of 900 kg/m^3 reduces to a bulk density of 550 kg/m^3 . The density of the propagating avalanche is estimated to 400 kg/m^3 . The avalanche was released by suddenly opening the flap. The model avalanche propagated down the chute slope and followed the local topography when leaving the generator-chute at 2200 m a.s.l.

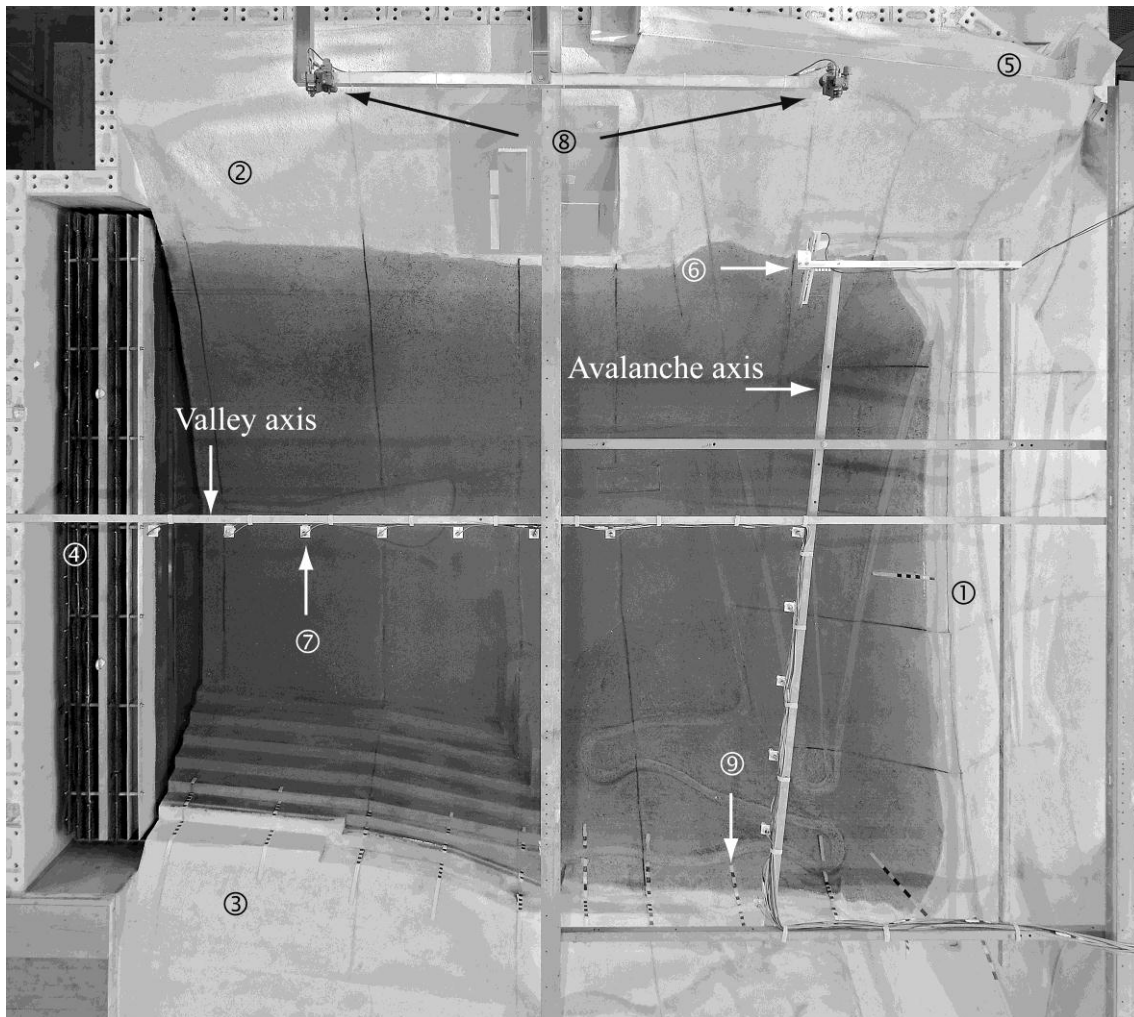


Figure 2. Situation of the physical model including ① dam, ② left valley flank, ③ right valley flank with stepped quarry, ④ wave absorber, ⑤ bearing of the avalanche generator-chute, ⑥ LDS, ⑦ UDS, ⑧ Video Cameras, ⑨ run-up markers.

The granulate material used for landslide modeling had a diameter of 8 mm and consisted of 13% polypropylene (PP) compounded with 87% of barium-sulfate, increasing both density and roughness. With a porosity of 45%, the grain density of 2430 kg/m^3 reduces to a bulk density of 1340 kg/m^3 . During slide propagation the density further decreases to an estimated value of 1100 kg/m^3 . A box equipped with a flap was used to keep the granulate on the topography until release. Specific wedge shaped insets configured the initial slide shape according to shear planes evaluated from numerical simulations. The slide was again released by suddenly opening the flap.

3 INSTRUMENTATION

Three measurement systems were applied (Fig. 2): (1) Laser Distance Sensors (LDS) to scan the avalanche shape prior to impact into the reservoir, (2) Ultrasonic Distance Sensors (UDS) to record the water surface elevation and (3) Digital Video Cameras to capture the wave run-up at the opposite shore-line and wave overtopping over the dam crest.

The LDS were mounted at an individual distance of 0.2 m and measured with a sample frequency of 100 Hz. By correlating the two slide profiles, the temporal offset was derived, relating to the slide impact velocity. Furthermore, the time origin $t = 0$ was specified for which the slide front impinged the reservoir surface.

The individual UDS were installed along two axes. During tests related to the snow avalanches, those axes were the main direction of the transferred impulse and the valley axis (Fig. 2). For landslide testing the wave properties were measured in the landslide axis as well as along an axis from the impingement point to the right dam abutment. Wave characteristics resulted from a correlation of single wave profiles of adjacent sensors. The UDS were operated with a sample frequency of 50 Hz.

Markers were attached on the topography along the right valley flank to allow for wave run-up height determination (Fig. 2). The exact values were derived visually by analyzing video sequences. The three cameras installed were connected to individual computers but controlled simultaneously with the further instrumentation, thus ensuring a thorough time assignment for all measurement systems.

4 SLIDE PARAMETERS

Since avalanche or landslide propagation may not be modeled correctly for the present model scale using the above described granular material, the impact parameters at FSL were considered exclusively. Those parameters were extracted from numerical simulations for the relevant avalanche and landslide (i.n.n. 2009), as listed in Table 1.

According to an evaluation conducted by TIWAG, the relevant avalanche has a gross volume of 90,000 m³, of which roughly 80,000 m³ enter the reservoir. The remaining volume deposits on the valley flank and on the dam embankment. The relevant avalanche has a density of 300 kg/m³, a thickness of 2 m and a front velocity of 23 m/s at FSL. During physical model tests, 15% of the material remained on the topography, the dam crest and the downstream dam face, resulting in 77,000 m³ eventually impinging the reservoir. The filtered avalanche profile scan is shown in Fig. 3a. The lower profile was already shifted for 1.14 s, such that its front coincides with the upper profile, resulting in a slide front velocity of roughly 23 m/s. The average slide thickness is assumed to be 2.0 m. Figure 3b compares the relative mass flux of the relevant avalanche at FSL with the mass flux derived from the numerical simulation, showing a good agreement.

Table 1. Relevant slide parameters of avalanche and landslide modeling, defined at reservoir impact.

Scenario	(1) Snow avalanche	(2) Landslide
Slide volume [m ³]	90,000	5000
Initial slide width [m]	260	31
Slide front velocity [m/s]	23	16
Slide thickness [m]	2	not specified

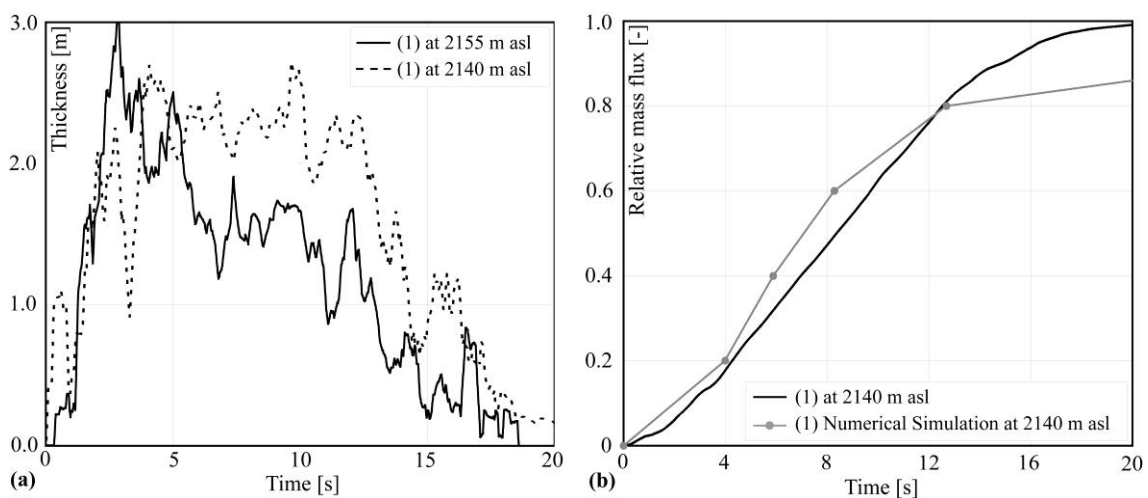


Figure 3. (a) Avalanche profile scans and (b) relative mass flux at FSL.

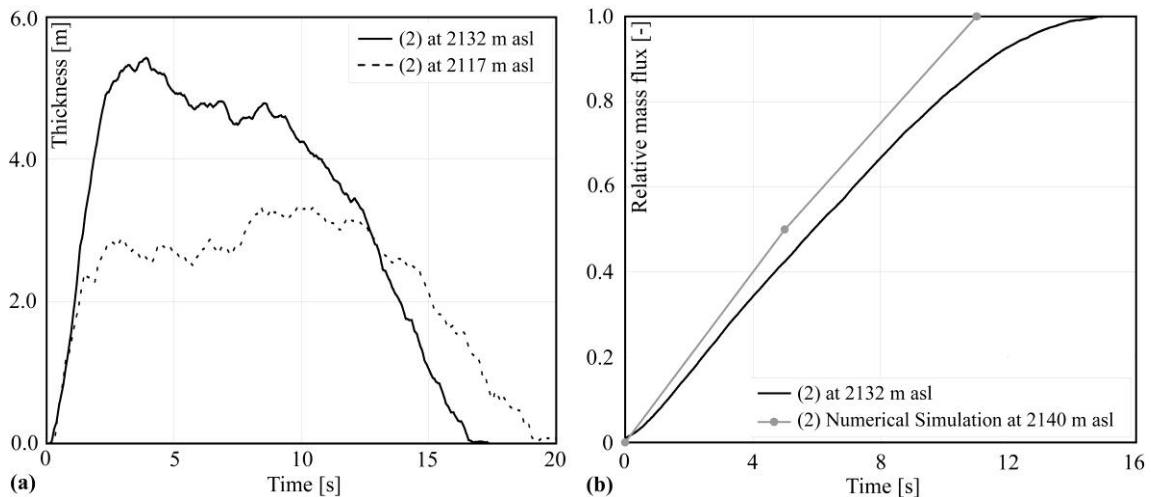


Figure 4. (a) Landslide profile scans and (b) relative mass flux at roughly FSL.

No precise values for landslide thickness and velocity were derived by TIWAG, hence modeling characteristics were compared to the numerical simulation in both, the relative mass flux and the slide width at roughly FSL. Since the unstable rock part is situated right above FSL, and LDS measurement is not applicable through the water surface, the slide characteristics were deduced from separate dry testing. The upper LDS was then installed at 2132 m a.s.l. and the lower at 2117 m a.s.l. Again, the slide front velocity was determined by slide front correlation of the two laser scans resulting in 17.6 m/s for the landslide event. The slide thickness is about 5.5 m (Fig. 4a) and the deduced mass flux coincides well with the numerical simulation (Fig. 4b). Whereas the slide propagated down to the reservoir bottom during dry testing, it remained on the valley flank due to buoyancy if the reservoir was filled. Reproducibility of the slide scenarios was verified by repetition of each test. Both slide and wave characteristics were found to be nearly identical.

5 RESULTS

5.1 Impulse waves

The resulting impulse waves are non-linear Stokes-type waves of transitional water-depth. With a wave length ranging from 200 to 500 m they have a celerity between 10 and 25 m/s. Due to the large width of the avalanche of 130 m, and the dam confining lateral wave propagation on the left side, a rather linear wave front is generated by the avalanche impact. Wave propagation thus occurs mainly two-dimensionally in the direction of the avalanche axis, with significantly smaller waves in the valley axis (Fig. 5). However, waves resulting from landslide impact propagate three-dimensionally and with significantly smaller heights, for instance $H_{(x=200\text{ m})} = 0.5\text{ m}$ for the landslide compared to $H_{(x=200\text{ m})} = 1.6\text{ m}$ of the avalanche generated waves, with H as the primary wave height and x as the radial distance to the impact point. Further wave parameters such as celerity or length are similar for both events.

Consecutive waves propagate with different celerity such that they tend to superpose each other resulting in increased wave height (see Figure 5, e. g. (1) valley axis, $x \approx 500\text{ m}$). The decreasing reservoir depth at the opposite shoreline results in increased impulse wave heights as a result of shoaling (Figure 5, (1) avalanche axis, $x \geq 350\text{ m}$).

5.2 Overtopping

Dam overtopping was not observed for any scenario, neither for avalanche nor for landslide impact. Solely at the right dam abutment a sparse wetting of the horizontal dam crest occurred. The downstream dam face remained completely dry throughout model test series of the relevant events.

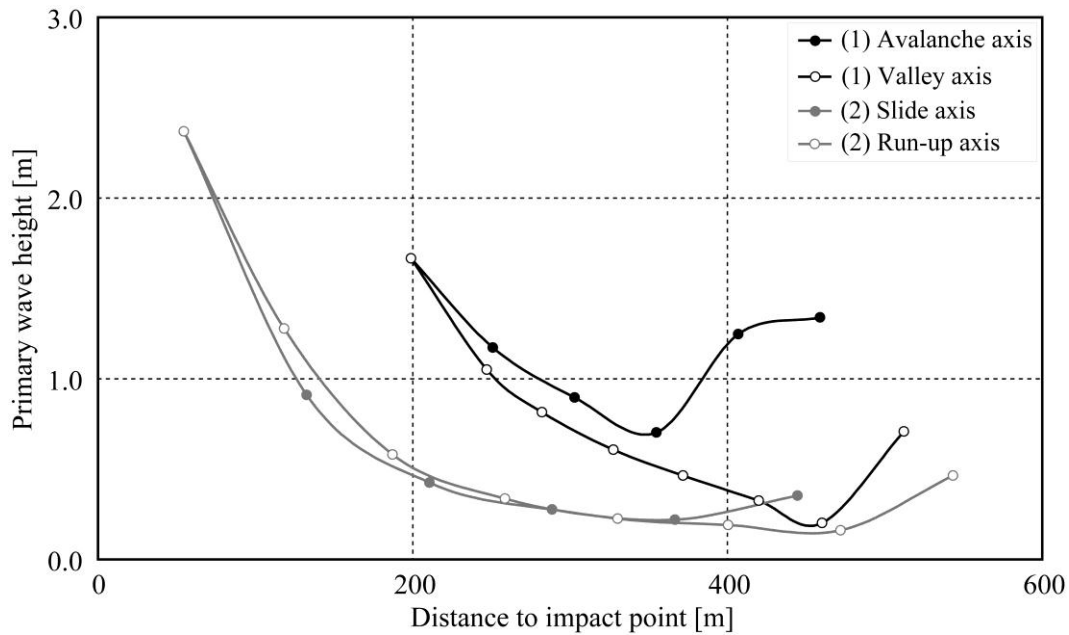


Figure 5. Measured primary wave heights for both measuring axes for (1) avalanche and (2) landslide scenario.

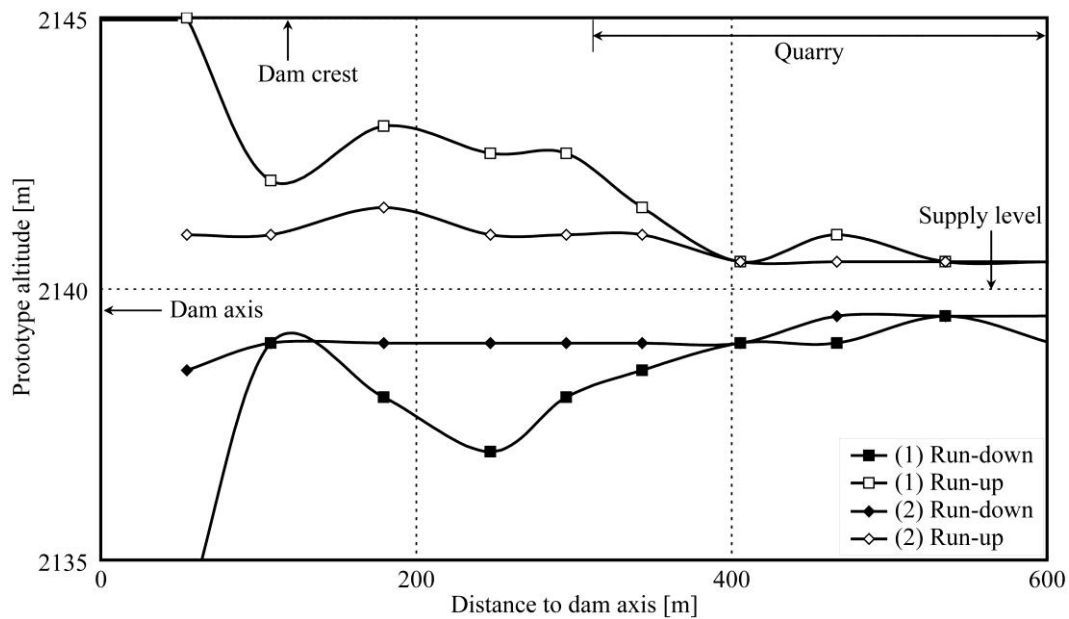


Figure 6. Maximum wave run-up and run-down measured at opposite shoreline during entire test period for (1) avalanche and (2) landslide scenario.

5.3 Wave run-up

Wave run-up and run-down were measured along the right shoreline using digital video recording. The maximum and minimum water levels within the observed period are shown in Figure 6 and refer to FSL. The abscissa represents the distance to the dam axis along the opposite shoreline with $x = 0$ at the dam; a planned quarry for dam construction material will be located at $x > 300$ m (Fig. 2, Fig. 6). The graphs represent maximum values observed during the test period of 170 s and do not stringently result from the primary wave. As described above, wave superposition may result in increased or decreased water levels, respectively. The maximum wave run-up of the relevant avalanche test was measured up to 5.0 m at the right dam abutment having the smallest slope angle of $\beta = 22^\circ$ of the investigated shore section. The deepest run-down reached to 2134 m a.s.l., i.e. was equivalent to 6.0 m below FSL. The steep shore slope at the

quarry further upstream, in combination with the smaller wave heights in the valley axis, result in significantly lower values for both run-up and run-down.

Due to the smaller height of landslide induced waves, wave run-up was smaller as well. The maximum values were measured to 1.5 m for both run-up and run-down.

6 COMPARISON TO PREDICTIONS

In order to facilitate a comparison, the analytical evaluation of impulse wave heights conducted by TIWAG was adapted to the specific physical model test conditions. This evaluation based on a VAW impulse wave guideline (Heller et al. 2009) is subdivided into three regions: (1) generation, (2) propagation and (3) run-up. The maximum wave height during wave generation is determined independently of 2D or 3D geometry. Thereafter, a distinction between 2D and 3D wave propagation is necessary, since for radially unconfined propagation the wave energy spreads in all directions, leading to smaller wave heights. The final computation of wave run-up is only dependent on wave parameters and the run-up shore angle. For the prediction of wave heights according to Heller et al. (2009), the slide centroid velocity is required in place of the slide front velocity deduced from numerical simulation or LDS scans. Following Volkart (1974), a reduction factor of 0.63, unfavorably selected on the safe side, was therefore applied to the slide front velocity of both events to estimate the slide centroid velocity.

As described above, avalanche generated impulse waves appeared to be mainly 2D and thus were compared to a 2D computation. The point of the maximum computed wave height ($H_M = 2.9$ m at $x_M = 75.4$ m) was beyond the instrumentation range, avoiding a direct comparison of measured and computed values. However, the extrapolated origin of the measured wave height roughly coincides with the computed maximum wave height (Fig. 7). The measured wave heights are significantly smaller than analytically predicted for the entire propagation area. Whereas the analytically estimated wave height is almost constant over the propagation distance, extensive wave height decay is observed in the model tests. The smallest wave height along the avalanche axis was measured to $H = 0.7$ m at $x \approx 350$ m, compared to a computed value of $H = 2.5$ m. A wave height increase due to shoaling is clearly visible in both graphs of Fig. 7, though the measured wave height in front of the opposite shore at $x \approx 450$ m is only $H = 1.34$ m compared to $H = 3.4$ m resulting from computation.

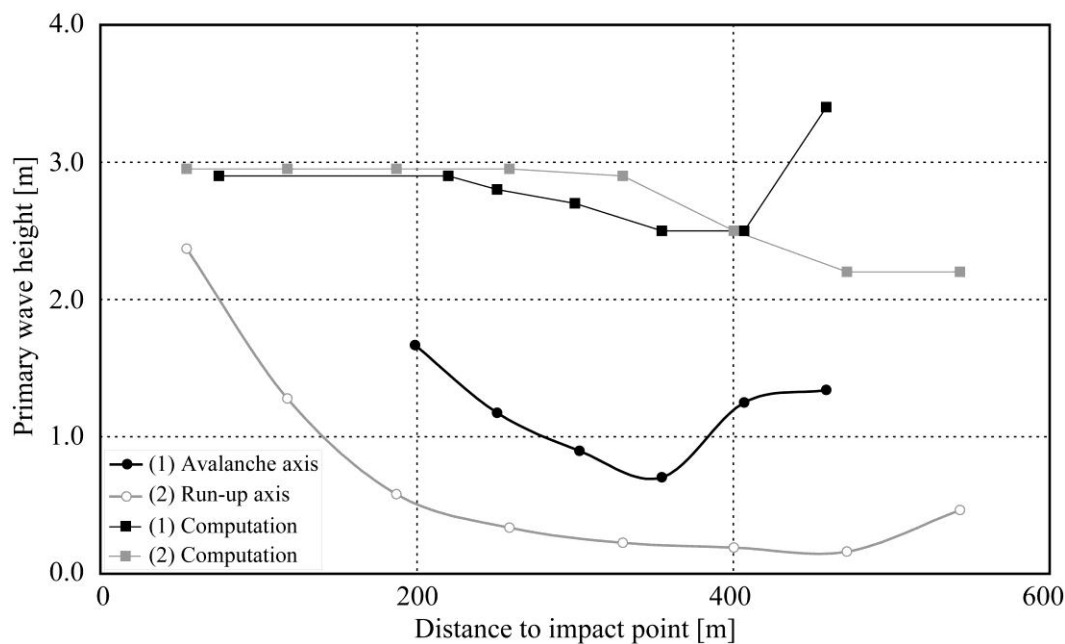


Figure 7. Comparison of computed and measured primary wave heights for (1) avalanche and (2) landslide scenario.

Since the landslide has a small width compared to the reservoir geometry, waves propagate unconfined, i.e. three-dimensionally. Measured wave heights were thus compared to a computation based on 3D propagation. Close to the impact point at $x \approx 50$ m a good correlation of measured ($H_M = 2.4$ m) and computed ($H_M = 3.0$ m) maximum wave heights in the generation zone is visible. Similar to the avalanches, the computed wave heights remain constant, contrary to the measured wave heights strongly decaying. The largest difference occurs at $x \approx 470$ m where the measured $H = 0.16$ m is about 14 times smaller than the predicted $H = 2.2$ m.

The wave run-up for avalanche impact was calculated to $R = 7.0$ m compared to $R = 5.0$ m measured during model testing (Fig. 6). For the landslide event the maximum run-up was calculated to $R = 4.2$ m contrary to the measured $R = 1.0$ m.

These relevant differences between estimation and measurements may be due to a number of not satisfied boundary conditions or so-called limitations of the computation according to Heller et al. (2009), resulting in a reduced validity of the prediction. Furthermore, effects of the complex highly 3D topography are difficult to include in the analytical evaluation.

7 CONCLUSIONS

The Kühtai reservoir in Tyrol, Austria, is planned in addition to the Sellrain-Silz group of HPPs. Due to its high alpine location, snow avalanche impact and resulting impulse waves must be considered in the dam safety assessment. Furthermore, a potential landslide region also possibly provoking impulse waves was determined. Since dam overtopping could not be excluded as a result of a preliminary analytical analysis, VAW was assigned to perform physical model tests.

These tests of the relevant scenarios showed that impulse wave run-up may reach the dam crest, however without dam overtopping even at full supply water level. The downstream dam face remained completely dry for the relevant avalanche and landslide tests. The results of the analytical evaluation were thus complemented, as a number of limitations were not satisfied during the computation procedure.

Eventually, TIWAG decided to further apply a 1.5 m high rock breakwater at the upstream dam crest, increasing the upstream dam slope to 1:1 in the upper part.

ACKNOWLEDGEMENTS

The authors kindly thank TIWAG for this interesting mandate and for the fruitful cooperation.

REFERENCES

- Boes, R., Hofer, B. & Perzmaier, S. 2007. Planung eines 120m hohen Steinschüttdammes im Zuge des Wasserkraftausbaus im Tirol. *Wasserwirtschaft* 97(10): 72-74 (in German).
- Dean, R.G. & Dalrymple, R.A. 2008. *Water wave mechanics for engineers and scientists, Advanced series on ocean engineering – 2*. Singapore: World Scientific.
- Heller, V., Hager, W.H. & Minor, H.-E. 2008. Scale effects in subaerial landslide generated impulse waves. *Experiments in Fluids* 44(5): 691-703.
- Heller, V., Hager, W.H. & Minor, H.-E. 2009. *Landslide generated impulse waves in reservoirs: Basics and computation, Mitteilungen 211*. R. Boes (ed.), Zurich: VAW, ETH Zurich.
- i.n.n. Ingenieurgesellschaft für naturraum-management mbH & Co KG 2009. *Lawinenmassendurchgang für eine Lawinenrutschdicke von 300 kg/m³*. Innsbruck: unpublished (in German).
- Volkart, P. 1974. Modellversuche über die durch Lawinen verursachten Wellenbewegungen im Ausgleichsbecken Ferden im Lötschental. *Wasser- und Energiewirtschaft* 66(8/9): 286-292 (in German).